Received: 4 September 2018 | Revised: 10 June 2020 | Accepted: 11 June 2020

DOI: 10.1002/mpr.1846

ORIGINAL ARTICLE

WILEY

Autism classified by magnetic resonance imaging: A pilot study of a potential diagnostic tool

Darko Sarovic[1,2] | Nouchine Hadjikhani[1,3] | Justin Schneiderman[2,4] | Sebastian Lundström[1] | Christopher Gillberg[1,5]

[1]Gillberg Neuropsychiatry Centre, Department of Psychiatry and Neurochemistry, Institute of Neuroscience and Physiology, Sahlgrenska Academy, University of Gothenburg, Gothenburg, Sweden

[2]MedTech West, Gothenburg, Sweden

[3]Department of Radiology, Athinoula A. Martinos Center for Biomedical Imaging, Harvard University, Charlestown, Massachusetts, USA

[4]Department of Clinical Neurophysiology, Institute of Neuroscience and Physiology, Sahlgrenska Academy, University of Gothenburg, Gothenburg, Sweden

[5]Institute of Health & Wellbeing, University of Glasgow, Glasgow, Scotland, UK

Correspondence
Darko Sarovic, Gillberg Neuropsychiatry Centre, Institute of Neuroscience and Physiology, Sahlgrenska Academy, University of Gothenburg, Gothenburg, Sweden.
Email: darko.sarovic@gu.se

Funding information
Vetenskapsrådet, Grant/Award Number: 2017-01359, 621-2012-3673; Avtal om Läkarutbildning och Forskning, Västra Götalandsregionen, Grant/Award Number: ALF-GBG716351; Barncancerfonden, Grant/Award Number: MT2014-007; Fredrik O Ingrid Thurings Stiftelse, Grant/Award Number: 2018-00419; Torsten Söderbergs Stiftelse, Grant/Award Number: M141/14

Abstract

Objectives: Individual anatomical biomarkers have limited power for the classification of autism. The present study introduces a multivariate classification approach using structural magnetic resonance imaging data from individuals with and without autism.

Methods: The classifier utilizes *z*-normalization, parameter weighting, and interindividual comparison on brain segmentation data, for estimation of an individual summed total index (TI). The TI indicates whether the gross morphological pattern of each individual's brain is in the direction of cases or controls.

Results: Morphometric analysis found significant differences within subcortical gray matter structures and limbic areas. There was no significant difference in total brain volume. A case-control pilot-study of TIs in normally intelligent individuals with autism (24) and without (21) yielded a maximal accuracy of 78.9% following cross-validation. It showed a high accuracy compared with machine learning methods when tested on the same dataset. The TI correlated well with the autism quotient ($R = 0.51$) across groups.

Conclusion: These results are on par with studies on autism using machine learning. The main contributions are its transparency and simplicity. The possibility of including additional neuroimaging data further increases the potential of the classifier as a diagnostic aid for neuropsychiatric disorders, as well as a research tool for neuroscientific investigations.

KEYWORDS
autism spectrum disorder, multivariate classification, structural magnetic resonance imaging, voxel-based morphometry

Abbreviations: ALL, all structural datasets; AQ, autism quotient; Ar, cortical ROI area; ASD, autism spectrum disorder; AUC, area under the curve; DSM, diagnostic and statistical manual of mental disorder; IQ, intelligence quotient; LOOCV, leave-one-out cross-validation; LUH, Lausanne University Hospital; ÖH, Östra Hospital; ROC, receiver operator characteristic; ROI, region of interest; SCV, subcortical gray matter volume; SUH, Sahlgrenska University Hospital; TD, typically developed; Th, cortical ROI thickness; TI, total index; UAR, unweighted average recall; WM, subcortical white matter volume.

1 | INTRODUCTION

Autism spectrum disorder (ASD) is characterized by difficulties in social communication, as well as repetitive and restricted behaviors and interests (American Psychiatric Association, 2013). Recent research on the neurobiology of ASD has targeted biomarker discovery that can aid in diagnostics. Having a biomarker as a compliment to the clinical interview could lower diagnostic costs, decrease the time until the individual receives a diagnosis, and potentially increase diagnostic accuracy. It could also help to define endophenotypes that can guide genetic research and evaluation of pharmacotherapy. The search for biomarkers in ASD casts a wide net. Proposed neuroanatomical biomarkers (Donovan & Basson, 2017; Ecker, 2017) include enlarged amygdalae (Sparks et al., 2002), increased cerebellar with decreased vermal size (Hardan, Minshew, Harenski, & Keshavan, 2001; Kaufmann et al., 2003), larger caudate nuclei (Hollander et al., 2005), atypical gyrification (Levitt et al., 2003; Piven et al., 1990), as well as changes in hippocampal volume and shape (Nicolson et al., 2006; Schumann et al., 2004). Functional neurophysiological biomarkers (Luckhardt, Jarczok, & Bender, 2014) include an increased excitation/inhibition ratio (Rubenstein & Merzenich, 2003), impairments in the mirror neuron system (Williams, Whiten, Suddendorf, & Perrett, 2001), local hyperconnectivity and global hypoconnectivity in coherence analyses (Belmonte et al., 2004; Catarino et al., 2013), and various changes in amplitude and timing of event-related potentials (Dawson, Webb, Carver, Panagiotides, & McPartland, 2004).

One reason for the many conflicting results in the neuroimaging of ASD is the heterogeneity of underlying causes and thus the phenotypic expression of the disorder, which necessitates identification of biologically relevant endophenotypes for deconstructing ASD (Bernhardt, Di Martino, Valk, & Wallace, 2017). Furthermore, neuroradiological studies have traditionally been hampered by manual segmentation and volumetry, which are not only time consuming (Collier et al., 2003) but also have high intra- and inter-operator variability (Despotovic, Goossens, & Philips, 2015). The advent of automated segmentation of the brain, using programs such as FreeSurfer (Fischl, 2012), has allowed researchers to segment and compare brains on a larger scale than previously possible with manual volumetry. This has allowed for the recent transition from single area volumetry to whole brain segmentation.

Attempts to reconcile the general principle of combining data from multiple biomarkers with the development of automated segmentation via factor analysis and machine learning have yielded varying amounts of success. Within the field of psychiatric neuroradiology, several machine learning paradigms have been utilized on combinations of data from magnetic resonance imaging, diffusion tensor imaging, and functional magnetic resonance imaging for classification (Orru, Pettersson-Yeo, Marquand, Sartori, & Mechelli, 2012). These include support vector machines (Ecker et al., 2010; Ecker et al., 2010; Ingalhalikar, Parker, Bloy, Roberts, & Verma, 2011; Libero, DeRamus, Lahti, Deshpande, & Kana, 2015; Uddin et al., 2011), generalized linear classifiers (Nielsen et al., 2013), logistic model trees (Jiao et al., 2010), and random forests (Zhou, Yu, & Duong, 2014).

The major strength of employing machine learning for classification is that one can analyze vast amounts of data both within and between modalities, thereby increasing the diagnostic yield of gathered data from participants. Despite this, many studies have utilized only one modality. It is likely, however, that not only the macroscopic gray matter structure, but also white matter tract thickness and connectivity pattern, as well as microscopic cytoarchitecture, functional neurophysiological aspects, and so on affect the expressed behavioral phenotype. Any complete functional model of the brain must therefore incorporate all such parameters. Recent studies utilize several modalities at once; one can expect that a greater proportion of future studies will follow this trend. For example, Libero et al. (2015) reported on a support vector machine implemented on combined magnetic resonance imaging, diffusion tensor imaging, and neurochemistry data that resulted in an accuracy of 91.9%, compared to Uddin et al. (2011)'s 88% and Ingalhalikar et al. (2011)'s 79% that were limited to one modality (magnetic resonance imaging and diffusion tensor imaging, respectively). Similarly, Zhou et al. (2014) implemented a random forest on structural and functional magnetic resonance imaging data with an accuracy of 70%, compared to Sabuncu et al's (2015) 59% using only structural magnetic resonance imaging.

Despite these advances, limitations in the existing literature include small sample sizes and lack of replication. Furthermore, several pitfalls specifically regarding the practical application of machine learning have also been noted (Bone et al., 2016; Kassraian-Fard, Matthis, Balsters, Maathuis, & Wenderoth, 2016). One of the most significant limitations to more widespread clinical use of machine learning is the need for a deep understanding of the theoretical underpinnings of machine learning, familiarity with the software, and rigorous testing of results in order to identify and correct errors such as overfitting. Such expertize is rarely available outside the computer science community. A transparent and easy-to-use statistical method for multivariate classification would therefore be more accessible to researchers outside the field of machine learning and, perhaps more importantly, to clinicians.

The aims of the present study were to develop a user-friendly multivariate statistical method for classification that does not rely on machine learning and apply it to brain magnetic resonance imaging segmentations in an attempt to classify a clinical case-control cohort. Herein, we present such a method and its implementation for classification of autism.

2 | METHOD

2.1 | Population

The sample consisted of 45 adult males (see Table 1): 24 autistic and 21 typically developed (TD) subjects, group matched for age and IQ. Exclusion criteria were IQ < 80 for both groups, the presence of any registered psychiatric diagnosis for the TD group, and comorbid Attention Deficit Hyperactivity Disorder (ADHD) for the ASD group. Informed consent forms were provided by all participants. The study

TABLE 1 Subject demographics, neuropsychological data, and macroscopic brain segmentation results

	ASD (mean ± SD)	TD (mean ± SD)	Student's *t*-test (*p*)
N	24	21	-
Age (years)	30.6 ± 7.1	28.2 ± 6.4	0.24
Full-scale IQ	109.8 ± 15.1	115.1 ± 11.2	0.21
AQ	23.0 ± 9.3	12.2 ± 7.0	0.00009*
White matter total (cm^3)	492.3 ± 55	459.6 ± 63	0.08
Gray matter total (cm^3)	696.6 ± 57	662.1 ± 57	0.06
Subcortical gray total (cm^3)	64.1 ± 5	58.2 ± 6	0.0009**
Brain total (cm^3)	1248.0 ± 115	1181.5 ± 114	0.06
Total intracranial volume (cm^3)	1687.3 ± 180	1576.0 ± 146	0.03*

Note: Data expressed as mean ± SD. Unpaired, two-tailed Student's *t*-test.

Abbreviations: AQ, autism quotient; ASD, autism spectrum disorder; IQ, intelligence quotient; TD, typically developing.

*$p < 0.05$; **significance level after Bonferroni correction within the family of macroscopic segmentations = 0.05/5 = 0.01.

was ethically approved by the regional ethical board in Gothenburg (DNR: 552-14).

TD cases were recruited from the website at the Gillberg Neuropsychiatry Centre (GNC; www.gnc.gu.se) and through flyers. All but one of the 24 ASD cases were recruited from two ongoing longitudinal studies at the GNC that have been described elsewhere (Davidsson et al., 2017; Helles, Gillberg, Gillberg, & Billstedt, 2015). Briefly, this is a well-characterized sample that has been longitudinally assessed, having been assigned a diagnosis of autism on at least two occasions, separated by at least 5 years, using the Diagnostic and Statistical Manual of Mental Disorder-4 (DSM; American Psychiatric Association, 1994) and the International Classification of Diseases-10 (World Health Organization, 1992). One patient was recruited via advertisement, and his medical records were obtained and scrutinized by an experienced senior child and adolescent psychiatrist to verify that diagnosis and exclusion criteria were met. All individuals in both groups were seen by a medical doctor and a psychologist. The TD subjects were screened for neurological and psychiatric disorders using a brief neurological examination and a medical/psychiatric checklist.

The participants also underwent intelligence testing (Wechsler Abbreviated Scale of Intelligence [Wechsler, 1999] or the Wechsler Adult Intelligence Scale-IV [Wechsler, 2008]) and completed the autism quotient (AQ; Baron-Cohen, Wheelwright, Skinner, Martin, & Clubley, 2001). IQ-test results were missing for two ASD cases and one TD case.

2.2 | Data acquisition

The participants' heads were scanned using 3-Tesla magnetic resonance imaging systems at three institutions using the recommended sequences for Freesurfer segmentation MPRAGE for Siemens, the MPRAGE equivalents FSPGR-BRAVO for GE, and TFE-SENSE for Philips. T1-weighted 3D-encoded images, consisting of 176 sagittal 1 mm slices, were used for the subsequent segmentation. The specific acquisition parameters are listed in Table 2.

TABLE 2 Acquisition parameters for magnetic resonance imaging scans

	SUH	ÖH	LUH
N	22	16	7
Sequence	TFE-SENSE	FSPGR-BRAVO	MPRAGE
Relaxation time (ms)	7600	2530	2530
Inversion time (ms)	600	1100	1100
Echo time (ms)	3.7	3.5	1.64/3.5/7.22
Flip angle	7°	10°	7°
Field-of-view (mm)	256	256	256

Abbreviations: LUH, Lausanne University Hospital; ÖH, Östra Hospital; SUH, Sahlgrenska University Hospital.

All scans were reviewed locally by a neuroradiologist for image quality and possible pathologic findings that, if present, were communicated to the participant and referred to the corresponding hospital for follow-up.

2.3 | Data processing

This study utilizes data generated by FreeSurfer (http://surfer.nmr.mgh.harvard.edu/) segmentations from the T1-weighted structural brain magnetic resonance imaging scans. FreeSurfer segmentation provides data about the volumes, areas (Ar), and thicknesses (Th) of cortical regions of interest (ROIs), as well as the volumes of subcortical gray matter (SCV) and white matter (WM) structures. The FreeSurfer recon-all pipeline with default settings was used to segment the brains. All FreeSurfer segmentations were visually inspected to ensure accurate cortical parcellations and subcortical segmentations. See Figures 1–3 for the parcellation (cortical ROIs) and segmentation

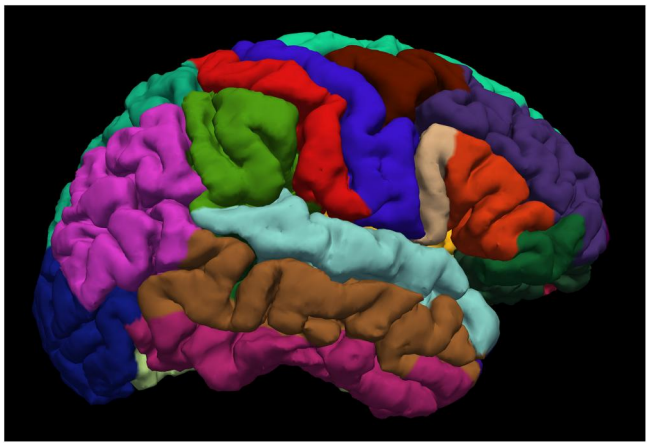

FIGURE 1 The FreeSurfer parcellation for a representative participant showing the lateral cortical regions of interest

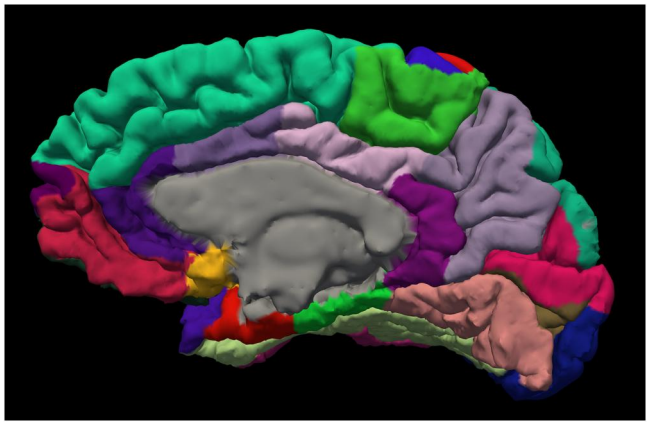

FIGURE 2 The FreeSurfer parcellation for a representative participant showing the medial cortical regions of interest

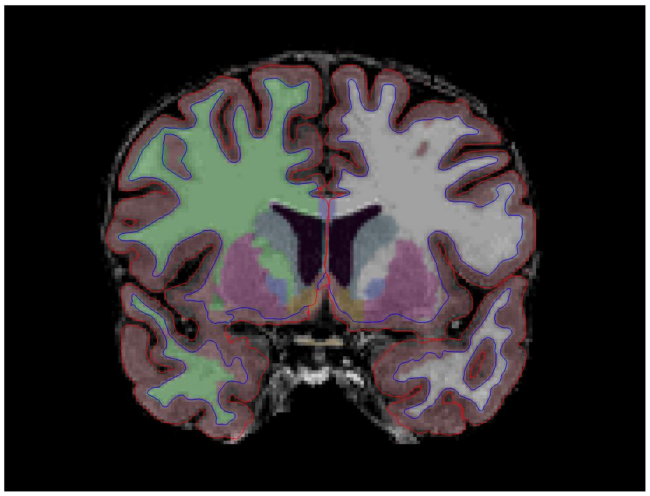

FIGURE 3 A coronal section of the T1-weighted sequence for a representative participant showing the labeling of subcortical regions of interest (mapped with different colors) following the FreeSurfer segmentation as well as the boundaries for the gray (red outline) and white matter (blue outline)

(subcortical ROIs) of a representative individual. The same FreeSurfer version (v5.3.0) and computer (MacOS 10.11.6) were used for all segmentations. All cortical parcellations were used. Specific segmentations were excluded as they were deemed irrelevant: WM and non-WM hypointensities, left and right vessel, optic chiasm, fifth ventricle, and left and right choroid plexus (see appendices for complete list of included data). The technical details have been explained in previous publications (Dale, Fischl, & Sereno, 1999; Fischl, Sereno, & Dale, 1999). The accuracy of FreeSurfer segmentations has been validated by both manual segmentation (Kuperberg et al., 2003) and histopathological specimens (Cardinale et al., 2014; Rosas et al., 2002). FreeSurfer is relatively insensitive to acquisition across platforms and magnetic resonance imaging manufacturers. Results are similar to within-scanner results (Han et al., 2006; Jovicich et al., 2009), with some brain areas showing lower variability (hippocampi and thalami) than others (amygdalae and accumbens areas; Morey et al., 2010).

2.4 | Statistical method used for analyzing segmented magnetic resonance imaging data

We employ the sign function (defined by Equation (1)) to determine which group average is larger for each given parameter (segmented ROI). We empirically use it to return $+1$ for those parameters for which the ASD group has a larger average size than the TD group and -1 for those for which it is smaller.

$$\mathrm{sgn}(\Delta g^p) = \frac{\mu^p_{\mathrm{ASD}} - \mu^p_C}{|\mu^p_{\mathrm{ASD}} - \mu^p_C|} \tag{1}$$

where Δg^p is the group difference for parameter p, and μ^p_{ASD} and μ^p_C are the averages for the ASD and TD groups respectively.

We define a weight for each parameter according to the square of its effect size (d^2) so that those parameters that have the greatest predictive value contribute the most to the total index (TI). The sign function is employed in order to maintain group directionality (i.e., positive for ASD and negative for TD) following the squaring of the effect size, which otherwise yields an absolute value. For a dataset with many parameters, one can manipulate the exponent of the effect size to increase diagnostic accuracy. By increasing the exponent, from the square to the cube for example, the weighting on the parameters that are more informative for the grouping increases. In other words, by increasing the exponent, the number of parameters that affect the TI decreases as it diminishes the importance of those parameters that are not significant in separating the groups relative to those that do. Not only integers, but also functions, such as the logarithm, can be used for effect size weighting.

$$d^2 = \mathrm{sgn}(\Delta g^p) \times \left| \frac{\mu^p_{\mathrm{ASD}} - \mu^p_C}{\mathrm{SD}^p_\mu} \right|^2 \tag{2}$$

The value of each parameter and participant is subtracted from the mean value of the groups for that parameter and Z-normalized

(first right-hand side term in Equation (3)). This enables all parameters to be of the same magnitude and thus directly comparable. We weight the parameters with the square of their respective effect size (Equation (2), last right-hand side term in Equation (3)) while maintaining their sign (Equation (1), middle right-hand side term in Equation (3)). As such, the sign determines the direction of each parameter (positive for ASD and negative for TD) and the magnitude is a measure of how group specific that parameter is for the participant; a large positive value for a parameter indicates that the size of the participant's ROI is in the direction of ASD and that the ROI has a distinct size difference between the groups. We calculate this for each parameter and subject:

$$X_n^p = \frac{x_n^p - \mu_\mu^p}{\mathrm{SD}_\mu^p} \times \mathrm{sgn}(\Delta g^p) \times d^2 \quad (3)$$

where X_n^p is the resulting normalized and weighted index value for parameter p and subject n compared to the mean of both groups. X_n^p is the weighted value of parameter p (there are q of these; for the case of all structural data, $q = 230$) for participant n (there are m of these; for the whole group analysis in this study, $m = 45$; when we run leave-one-out cross-validation [LOOCV], $m = 44$). μ_μ^p is the average value between the group averages for the parameter in question (μ^p, or the average of parameter p across all subjects, is used if group sizes are equal). μ_{ASD}^p and μ_C^p are the group averages for ASD and TD groups for each parameter p.

The sum of the index values for each parameter is calculated by

$$\mathrm{TI}_n = \sum_{p=1}^{q} (X_n^p) \quad (4)$$

to generate the total index, TI_n, for subject n.

In general, TI is a singular measure of an individual's position in a spectrum of multidimensional parameter spaces collapsed onto one axis. Those parameters that best separate the groups add the most to the TI while those that do not separate the groups have little, if any, contribution to it. The TIs for our dataset summarize the pattern of brain volumes and thicknesses for each participant in relation to the sample as a whole. The midpoint between the group averages, $\mathrm{TI} = 0$, represents a standard cutoff value for classification. The TIs for this dataset—based only on magnetic resonance imaging segmentation measures—are a quantification of how "autism-like" each brain is, with positive values representing an autistic-like pattern. Thus, employing a diagnostic cutoff of $\mathrm{TI} > 0$ increases specificity and decreases sensitivity. An example spreadsheet with the statistical method and information regarding it are found in the Supplementary materials 1 and 2.

2.5 | LOOCV and performance metric

The exhaustive form of leave-p-out cross-validation, LOOCV, was used for the determination of diagnostic accuracy of the method. It entails calculation of parameter averages, standard deviations, and effect sizes of the case and control groups, as presented in Section 2.4, with one participant excluded. The method is then applied to that participant to yield the TI of the "unknown" participant. In other words, the testing set is separated from the training set. This process was iterated for each of the 45 participants in the study, and for each of the datasets and all datasets together.

We use the unweighted average recall (UAR), which is the arithmetic mean of the values for specificity and sensitivity, as a performance metric. For unequally sized groups, this metric is preferable over accuracy, since it places equal weight on both specificity and sensitivity.

Linear regression was performed on the TI and AQ data and the Pearson's R, coefficient of determination (R^2), and statistical significance are presented.

2.6 | Comparison with machine learning methods

Four different machine learning algorithms were applied on the segmentation data (all datasets: parcellations and segmentations using FreeSurfer [see appendices for complete list]) to compare classification accuracies with the presented method: decision tree classifier, support vector machine, logistic regression, and neural network. They were implemented using the Python-based Scikit-learn module (Pedregosa et al., 2011). Although a neural network is not expected to work well for segmented, preprocessed data and small sample sizes, it was included for completion. LOOCV was used to predict the diagnostic status of the left-out individual, and the percentage of correct classifications for each method was calculated following 5000 iterations of training and testing (a 44/1 split for training/testing with split randomization and no random seed for training).

3 | RESULTS

3.1 | Behavioral phenotype

The average AQs for the ASDs and TDs were similar to previous reports in the literature (Lugnegard, Hallerback, & Gillberg, 2015; Ruzich et al., 2015) with 23.0 ± 9.3 and 12.2 ± 7.0, respectively ($p = 0.00009$, $d = 1.31$). Table 3 shows the linear regression results between AQ and cross-validated TIs for each of the data sets. Figure 4 illustrates the correlation using SCV data, including the regression line.

3.2 | Brain segmentation results

Following Bonferroni correction within the family of macroscopic segmentations (total intracranial volume, brain volume, cortical gray matter volume, WM, and SCV; $p < 0.01$), only SCV achieved significance ($p = 0.0009$). The results of the macroscopic segmentations are listed in Table 1. Segmentation results with group averages

TABLE 3 Linear regression results for total index using different data sets and the autism quotient

Data set	*R*	R^2	*p*	*F*-test
SCV	0.51	0.26	<0.0005	$F(1,43) = 15.140$
Th	0.16	0.03	0.28	$F(1,43) = 1.192$
Ar	0.37	0.14	0.01	$F(1,43) = 6.869$
WM	0.35	0.12	0.02	$F(1,43) = 6.096$
All data	0.44	0.19	0.003	$F(1,43) = 10.089$

Note: Pearson's *R*, R^2, and significance level are presented for the linear correlation between the total index for different data sets and the autism quotient.

Abbreviations: Ar, cortical area; SCV, subcortical volume; Th, cortical thickness; WM, white matter volume.

and significance values can be found for SCV, Th, Ar, and WM in Appendices A–D, respectively. For these segmentations, group differences were apparent after Bonferroni correction for several ROIs.

Within the family of SCV, the ASD group had enlarged hippocampi bilaterally, right thalamus, and left nucleus pallidus. From the cortical ROIs, significant differences in thickness were found for the left caudal anterior, and rostral anterior cingulate gyrus, right fusiform gyrus, bilateral entorhinal gyri, right parahippocampal gyrus, right inferior and superior temporal gyri, as well as the pericalcarine gyri bilaterally. For Ar, only the inferior temporal gyri bilaterally and the left banks of the superior temporal sulcus achieved significance. No WM segmentations were significantly different following Bonferroni correction.

3.3 | Overall classifier performance

The method was applied both on individual FreeSurfer segmentations (SCV, Th, Ar, and WM) and all the datasets together. The resulting TI values were statistically compared and the results are presented in Table 4. Figure 5 shows the receiver operator characteristic (ROC) curve, including area under the ROC (AUC), for each dataset. Figure 6 shows the TIs of the individuals using all structural data, together with group averages (ASD: 30.5 ± 32.7, C: −30.5 ± 41.4) and 95% confidence intervals (ASD: 15.0, C: 21.0).

The greatest diagnostic accuracies were obtained using individual structural datasets (SCV, Ar, and WM), while the greatest effect sizes and significance levels were obtained from SCV and all datasets combined. The AUC was highest for SCV and all datasets showing that they confer the greatest diagnostic accuracy across the spectrum of TIs.

Compared with the machine learning methods (see Table 5), the present method was minimally outperformed only by the decision tree classifier (accuracy 67.5% compared with 66.1%). However, when optimizing the cutoff value, it outperformed all the algorithms (73.2%). The optimization of the cutoff value (selection of a threshold for the TI that produces the highest accuracy) was performed with one individual excluded (using the TIs for $n-1$ subjects), so one cannot expect a "learning" effect.

4 | DISCUSSION

Individuals in our study were classifiable as having autism or not with high accuracy using only the pattern of gray matter sizes from structural brain magnetic resonance imaging. It is our belief that the potential of this method is considerable, and that this study acts as a proof-of-concept that one could classify psychiatric disorders neuroradiologically, even when dealing with such a heterogeneous disorder as ASD. ASD is a neurodevelopmental disorder with subtle diffuse neuroanatomical differences, and for such disorders, one cannot expect individual ROIs or neurophysiological biomarkers to have particularly good predictive values at the individual level, which is why multivariate models outperform univariate models in terms of prediction (Sabuncu et al., 2015).

The performance of the current method could be further improved by incorporating data about white matter and functional neurophysiology, somatic biomarkers, and behavioral questionnaires; any quantitative measure that reliably differentiates between ASDs and TDs can be implemented to increase its diagnostic accuracy.

Our present morphometric results are mostly in line with previous research. A review by Amaral, Schumann, and Nordahl (2008) showed that although children tend to have larger total brain, gray and white matter volumes, these tend to normalize toward adulthood. Our results for these measures were insignificant following Bonferroni correction. Also, we did not find the corpus callosum to be smaller in ASDs, as in previous studies (Bellani, Calderoni, Muratori, & Brambilla, 2013). Moreover, specific cortical ROIs that we found to have altered thicknesses and areas (see Appendices A–C, respectively) correspond well both to those in other neuroanatomical studies, as well as to the ROIs that have been implicated in neurophysiological and histopathological studies. The relevant differences identified in this study clustered around the cingulate gyrus, temporal cortex (including the fusiform and entorhinal gyri), and the parahippocampal gyrus, all of which are parts of the limbic cortex. The limbic system and temporal cortex have consistently been shown to be impacted in ASD.

A comment regarding the discrepancy in the classification results using all or individual datasets is warranted. Using SCV, Ar, and WM data alone in the classification yielded higher diagnostic accuracy compared to when used in conjunction with all datasets, perhaps due to the particularly poor discrimination by Th data where the group TIs overlap (see Figure 5). This could indicate the presence of different anatomical endophenotypes in our sample; we did not, however, have enough power to perform subgroup analyses. It could also represent an idiosyncrasy due to the small sample size, which is another reason to include a larger sample in a replication study. Given that the SCV dataset had the highest correlation to the AQ, it is possible that this represents a behavioral endophenotype.

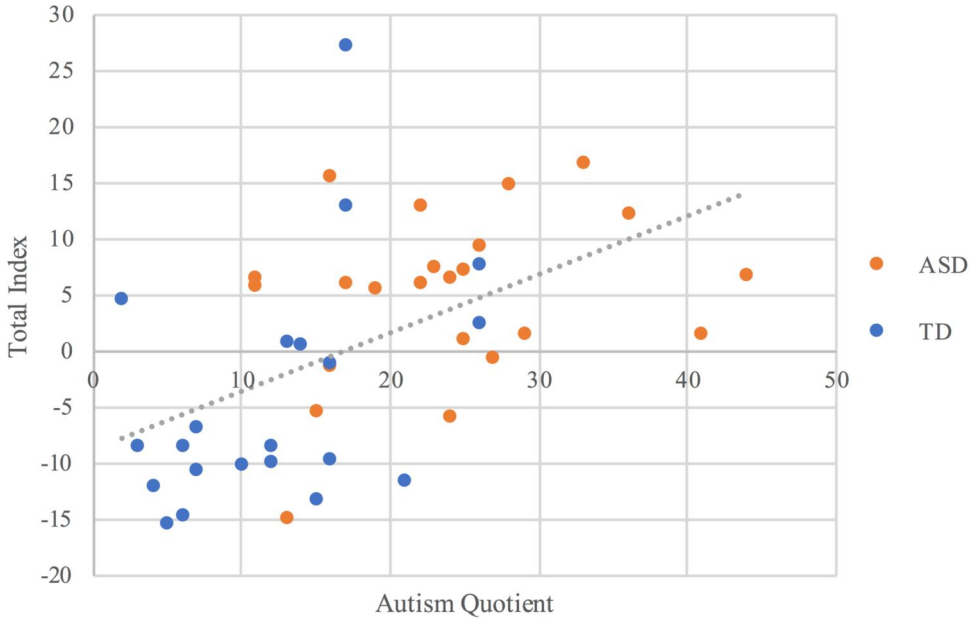

FIGURE 4 The total index (TI), based on subcortical volume data (SCV), and the autism quotient (AQ) showed a moderate statistically significant correlation ($F(1,42) = 15.140$, $p < 0.0005$), with an R^2 of 0.26. Removal of the typically developing (TD) outlier (a residual of 3.11 standard deviations from the regression line) slightly improved the regression results ($F(1,43) = 19.687$, $R^2 = 0.32$, $p < 0.0005$). ASD, autism spectrum disorder

TABLE 4 Statistical results for TI values obtained following LOOCV

Dataset	Student's *t*-test (*p*)	Cohen's *d*	AUC	UAR (%)[a]	Maximal UAR (cutoff)[b]
SCV	0.0013	0.98	0.792	72.9	78.9% (−6)
Th	0.0026	0.88	0.732	66.4	72.6% (−5)
Ar	0.026	0.60	0.742	75.6	77.7% (−1)
WM	0.050	0.50	0.714	75.9	75.9% (0)
All data	0.0013	0.95	0.789	66.1	73.2% (12)

Note: Unpaired, one-tailed Student's *t*-test.

Abbreviations: Ar, cortical area; AUR, area under curve; LOOCV, leave-one-out cross-validation; SCV, subcortical volume; Th, cortical thickness; TI, total index; UAR, unweighted average recall; WM, white matter volume.

[a]UAR presented using a standard cutoff value of TI = 0.

[b]Maximal UAR obtained when optimizing the cutoff value for TI to yield the highest UAR.

4.1 | Limitations of the study

Our sample was not population based, which could inflate diagnostic accuracy due to lower than normal variation. The TD group had similar AQs as other TD groups in previous research. However, the AQs for our ASD cases was similar to, or lower than those of previous studies, which might reflect a milder phenotype and thus underestimate the results. As with previous studies, ours has a rather small sample, and replications of the present method should aim to include larger samples for more robust baselines with which to compare potential patients; this would also improve sampling issues. Furthermore, the classification was only used on a sample with autism. As such, conclusions about its specificity for autism cannot be drawn definitively. Further work should include a sample with other neurodevelopmental disorders on which our method can be applied in order to ensure that it does not classify neurodevelopmental disorders in general, rather than ASD specifically. Since we did not include individuals with IQ < 80, generalization of these results to that group is precluded. Due to differences in neuroanatomy between the sexes (Lenroot & Giedd, 2010), females were not included. Moreover, the sample only included adult participants. The continuous brain development throughout childhood leads to higher interindividual variation. Given that autism is often diagnosed at an early age, it would be interesting to investigate how the method would perform on a very young sample. However, less stable diagnoses and differing neurodevelopmental trajectories require larger sample sizes than doing the same for adults. Finally, despite studies showing the reliability of FreeSurfer segmentation results across pipelines, a potential issue is that several imaging centers were used in this study. It would have been preferable to use one imaging center

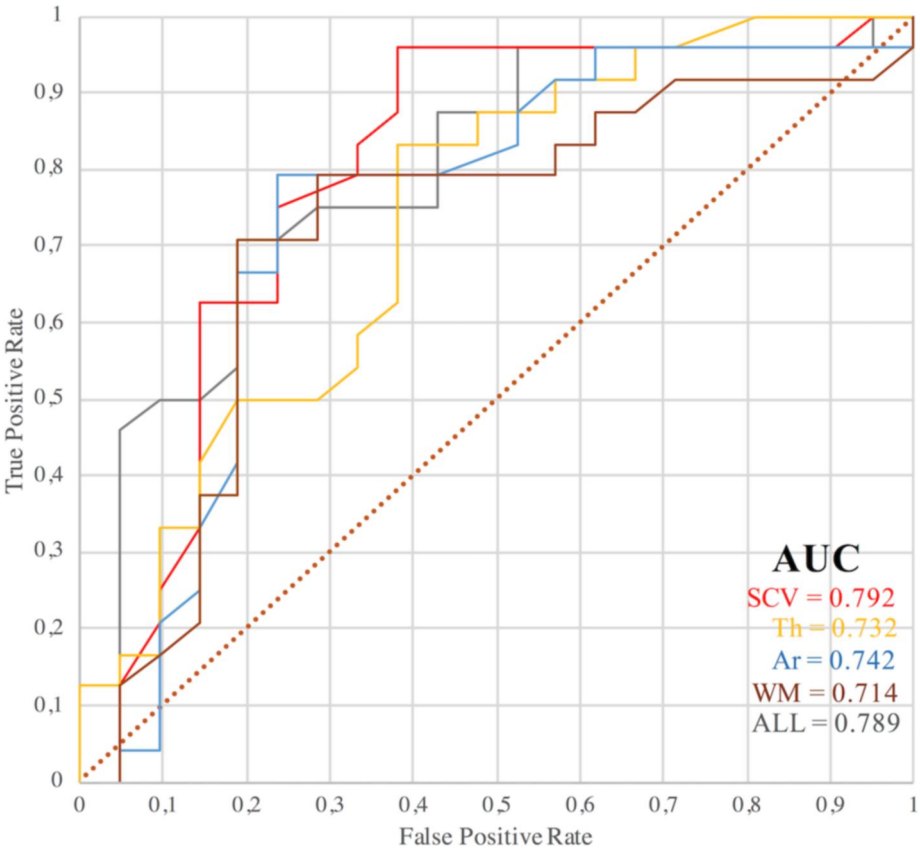

FIGURE 5 Receiver operating characteristic (ROC) showing the area under the curve (AUC) for cross-validated total indices using different data sets. ALL, all structural data sets; Ar, cortical area; SCV, subcortical gray matter volume; Th, cortical thickness; WM, white matter volume. The dashed red line represents a chance probability of 50%

or to regress out site effects. Unfortunately, since these data were recorded before the development of the method, the groups were not site matched, which precludes the use of regression analysis, lest one also regress out the effect of the presence of diagnosis. We recommend that a replication study should aim to employ a homogenous data acquisition and analysis pipeline to reduce the possible influence of random error. On the other hand, positive findings across centers points to the robustness of the neuroanatomical differences between the groups.

4.2 | Use in the study of ASD

A currently unsolved issue complicating research surrounding ASD in general, and its neuroimaging in particular, is the fact that it lacks both biological and construct validity (Waterhouse, London, & Gillberg, 2017); there is no agreed upon brain-based model of ASD and the behavioral symptoms have been found to be highly heterogeneous across patients. Until subgroups of ASD have been identified and defined, this will remain a limiting factor for the field. A further complicating issue is that inter-rater reliability of the diagnosis is less than 100%. Any classification system is intricately dependent on the validity of the clinical diagnosis, and it would be a logical fallacy to assume that a classification system can outperform the clinical interview, given that the classification grouping is based on the clinical diagnosis.

The heterogeneity in ASD is a complication for multivariate analyses, such as this one, especially with small sample sizes. Defining subgroups of autism is central to ASD diagnostics in general and also of importance if brain-based classification systems are to be accurate enough at the individual level. Given that subgroups of ASD have different neuroanatomical patterns, actual case-control differences from multivariate analyses will be underestimated. One way to minimize this effect would be to standardize the clinical diagnostic procedure; if possible, the same psychiatrist should diagnose all included cases, as in this sample. Furthermore, a majority of patients with ASD have neuropsychiatric comorbidities, such as ADHD. Such patients were excluded in the present study. However, given the clinical overlap of neuropsychiatric disorders, a replication study with pairwise comparison of cases with autism, ADHD, and both is necessary to determine specificity of the method, and hence its clinical relevance.

The TI from this method is a continuous variable that resembles the nondichotomous clinical expression of ASD and allows for correlational studies with regard to clinical data. Ecker et al. (2010) were the first to show a correlation between the results of a

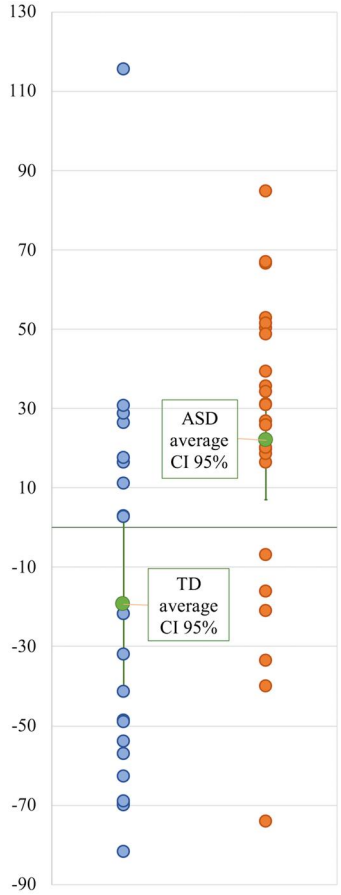

FIGURE 6 Total index values for all participants using all segmentation data sets. The figure shows the group averages with error bars representing 95% confidence intervals (CIs). ASD, autism spectrum disorder; TD, typically developed

TABLE 5 Classification results, following LOOCV, for machine learning algorithms when applied on all structural datasets (parcellations and segmentations from FreeSurfer)

Method	Classification accuracy (%)
Presented classification method	66.1 (73.2% maximal UAR)
Decision tree classifier	67.5
Support vector machine	56.8
Logistic regression	58.1
Neural network (multilayer perceptron)	53.6

Abbreviations: LOOCV, leave-one-out cross-validation; UAR, unweighted average recall.

multivariate analysis and the AQ. Using gray matter data, they found correlations of 0.51 and 0.22 for the left and right hemispheres, respectively. Using SCV, we also found a moderate correlation with AQ ($R = 0.51$). Other studies have done the same for other behavioral measures, such as the Autism Diagnostic Interview and the Autism Diagnostic Observation Schedule, and by making the comparison between multivariate analyses and questionnaires one can make them more objective and show their biological validity.

Macrocephaly in ASD has been associated with regressive symptoms and low IQ (Amaral et al., 2017). Since this sample had normal IQ and no significant brain volume difference, normalization for brain volume was not performed. Even though the macroscopic segmentations in this study (except SCV) did not reach significance, a frequent neuroanatomical finding in ASD is an increased intracranial volume. A replication study using a population-based sample could shed light on whether these findings are due to sampling differences. The question of regressing out intracranial or brain volume for ASD remains open, since in doing so, one could remove the effect of a rather stable neuroanatomical biomarker. The loss of information must be weighed against what is gained, and the decision will ultimately depend on the specific classification method employed and whether or not it improves its accuracy.

4.3 | Applicability of the method on other psychiatric conditions

A possible future direction is to use the method as a general diagnostic aid. By compiling data from several disorders, one can apply the method on an individual for each disorder to get a neurological profile based on disorder-specific TIs and develop best fits for different disorders (like a risk profile), as well as for behavioral measures in the healthy population, such as personality traits. This would be similar to how the Mini-International Neuropsychiatric Interview (Sheehan et al., 1998) and the Structured Clinical Interview for DSM (First, Williams, Karg, & Spitzer, 2015) are being used currently during initial psychiatric assessments to guide further evaluations, but from an objective neurobiological viewpoint rather than from self-report questionnaires.

4.4 | Methodological discussion

Rather than just being a binary classifier, the outcome measure (TI) is a continuous variable. This is beneficial since it gives a probabilistic estimate of the association with the underlying disorder and allows for correlational studies to be performed.

Utilization of machine learning methods requires specific expertize, limiting its practical usability, and rendering it unavailable to most scientists and clinical practitioners. The presented method requires only elementary mathematical knowledge and a spreadsheet, making it widely available. Despite this, the diagnostic accuracy of the present method is comparable to studies using machine learning on neuroimaging data: a maximal cross-validated classification accuracy of 78.9% compared to 59%–88% for studies using magnetic resonance imaging.

Careful consideration of the underlying neurobiology should be made regarding the choice of parameter selection. For example, since

the function of white matter tracts more closely relates to tract thickness and connectivity than to the volume of a particular white matter segment, utilization of diffusion tensor imaging data may yield superior results compared with segmentation data. Similarly, some cortical parcellations (e.g., V1, primary motor cortex, and Broca's area) rest on logical assumptions about underlying function, and as such parcellated data may yield higher accuracies than pure voxel-based analyses.

Previous studies have shown improvements in classification accuracy for ASD both when using functional data, as well as when using several modalities at once, lending credence to the potential of further improvement of this method with the inclusion of functional neurophysiological data.

While FreeSurfer segmentation data have been shown to be reliable, any analysis pipeline includes several steps (acquisition, preprocessing, and segmentation), each of which can induce small errors. As such, it is advisable that the pipeline within a study be standardized. In line with this, the previous studies with the lowest UAR (Nielsen et al., 2013; Sabuncu et al., 2015) were the ones using data from open databases containing data with different acquisition pipelines.

4.5 | Recommendations for future multivariate analyses

Based on the reasoning above, we recommend that future studies attempting multivariate analysis (1) include larger sample sizes, (2) focus on well-defined patient cohorts, preferably diagnosed by the same physician (at least for heterogeneous disorders such as ASD), (3) test the method on another clinical sample (e.g., another neuropsychiatric disorder if investigating ASD) to assess its specificity, (4) include clinically relevant behavioral data, with which classification results can be compared, and that can potentially also be used in the analysis, (5) employ a standardized data acquisition pipeline that is up-to-date regarding hardware and software versions, (6) utilize several imaging modalities at once, and (7) base the selection of parameters on careful consideration of the underlying neurobiological processes for each disorder.

5 | CONCLUSION

Our method was utilized on magnetic resonance imaging data and yielded a maximal diagnostic accuracy of 78.9% for ASD when compared to the clinical interview, which is the gold standard of clinical diagnosis. The main contribution of this study is the development of a novel and simple multivariate classification method that requires limited specific expertize without sacrificing diagnostic accuracy in comparison with machine learning methods. This study adds to previous studies indicating it might be an achievable goal to classify psychiatric disorders—even such a heterogeneous disorder as ASD—using neuroimaging methods.

ACKNOWLEDGEMENTS

The authors would like to thank Noreen Ward for her help regarding FreeSurfer. This work was supported by Vetenskapsrådet (grant number 2017-01359; 621-2012-3673), ALF (grant number ALF-GBG716351), Barncancerfonden (MT2014-007), Fredrik O Ingrid Thurings Stiftelse (2018-00419), and Torsten Söderbergs stiftelse (grant number M141/14). Other than financial support, there was no involvement in the study.

CONFLICT OF INTEREST

The authors declare that they have no conflict of interest.

ORCID

Darko Sarovic https://orcid.org/0000-0002-9302-4890
Nouchine Hadjikhani https://orcid.org/0000-0003-4075-3106
Justin Schneiderman https://orcid.org/0000-0002-4441-2360
Sebastian Lundström https://orcid.org/0000-0001-7235-8499
Christopher Gillberg https://orcid.org/0000-0001-8848-1934

REFERENCES

Amaral, D. G., Li, D., Libero, L., Solomon, M., Van de Water, J., Mastergeorge, A., … Wu Nordahl, C. (2017). In pursuit of neurophenotypes: The consequences of having autism and a big brain. *Autism Research*, *10*(5), 711–722. https://doi.org/10.1002/aur.1755

Amaral, D. G., Schumann, C. M., & Nordahl, C. W. (2008). Neuroanatomy of autism. *Trends in Neurosciences*, *31*(3), 137–145. https://doi.org/10.1016/j.tins.2007.12.005

American Psychiatric Association. (1994). *Diagnostic and statistical manual of mental disorders* (4th ed.). Arlington, VA: American Psychiatric Publishing.

American Psychiatric Association. (2013). *Diagnostic and statistical manual of mental disorders* (5th ed.). Arlington, VA: Americal Psychiatric Publishing.

Baron-Cohen, S., Wheelwright, S., Skinner, R., Martin, J., & Clubley, E. (2001). The autism-spectrum quotient (AQ): Evidence from asperger syndrome/high-functioning autism, males and females, scientists and mathematicians. *Journal of Autism and Developmental Disorders*, *31*(1), 5–17.

Bellani, M., Calderoni, S., Muratori, F., & Brambilla, P. (2013). Brain anatomy of autism spectrum disorders I. Focus on corpus callosum. *Epidemiology and Psychiatric Sciences*, *22*(3), 217–221. https://doi.org/10.1017/S2045796013000139

Belmonte, M. K., Allen, G., Beckel-Mitchener, A., Boulanger, L. M., Carper, R. A., & Webb, S. J. (2004). Autism and abnormal development of brain connectivity. *Journal of Neuroscience*, *24*(42), 9228–9231. https://doi.org/10.1523/JNEUROSCI.3340-04.2004

Bernhardt, B. C., Di Martino, A., Valk, S. L., & Wallace, G. L. (2017). Neuroimaging-based phenotyping of the autism spectrum. *Current Topics in Behavioral Neurosciences*, *30*, 341–355. https://doi.org/10.1007/7854_2016_438

Bone, D., Bishop, S. L., Black, M. P., Goodwin, M. S., Lord, C., & Narayanan, S. S. (2016). Use of machine learning to improve autism screening and diagnostic instruments: Effectiveness, efficiency, and multi-instrument fusion. *Journal of Child Psychology and Psychiatry*, *57*(8), 927–937. https://doi.org/10.1111/jcpp.12559

Cardinale, F., Chinnici, G., Bramerio, M., Mai, R., Sartori, I., Cossu, M., … Ferrigno, G. (2014). Validation of FreeSurfer-estimated brain cortical thickness: Comparison with histologic measurements. *Neuroinformatics*, *12*(4), 535–542. https://doi.org/10.1007/s12021-014-9229-2

Catarino, A., Andrade, A., Churches, O., Wagner, A. P., Baron-Cohen, S., & Ring, H. (2013). Task-related functional connectivity in autism spectrum conditions: An EEG study using wavelet transform coherence. *Molecular Autism*, *4*(1), 1. https://doi.org/10.1186/2040-2392-4-1

Collier, D. C., Burnett, S. S., Amin, M., Bilton, S., Brooks, C., Ryan, A., … Starkschall, G. (2003). Assessment of consistency in contouring of normal-tissue anatomic structures. *Journal of Applied Clinical Medical Physics*, *4*(1), 17–24. https://doi.org/10.1120/1.1521271

Dale, A. M., Fischl, B., & Sereno, M. I. (1999). Cortical surface-based analysis. I. Segmentation and surface reconstruction. *NeuroImage*, *9*(2), 179–194. https://doi.org/10.1006/nimg.1998.0395

Davidsson, M., Hult, N., Gillberg, C., Sarneo, C., Gillberg, C., & Billstedt, E. (2017). Anxiety and depression in adolescents with ADHD and autism spectrum disorders; correlation between parent- and self-reports and with attention and adaptive functioning. *Nordic Journal of Psychiatry*, *71*(8), 614–620. https://doi.org/10.1080/08039488.2017.1367840

Dawson, G., Webb, S. J., Carver, L., Panagiotides, H., & McPartland, J. (2004). Young children with autism show atypical brain responses to fearful versus neutral facial expressions of emotion. *Developmental Science*, *7*(3), 340–359.

Despotovic, I., Goossens, B., & Philips, W. (2015). MRI segmentation of the human brain: Challenges, methods, and applications. *Computational and Mathematical Methods in Medicine*, *2015*, 450341. https://doi.org/10.1155/2015/450341

Donovan, A. P., & Basson, M. A. (2017). The neuroanatomy of autism—A developmental perspective. *Journal of Anatomy*, *230*(1), 4–15. https://doi.org/10.1111/joa.12542

Ecker, C. (2017). The neuroanatomy of autism spectrum disorder: An overview of structural neuroimaging findings and their translatability to the clinical setting. *Autism*, *21*(1), 18–28. https://doi.org/10.1177/1362361315627136

Ecker, C., Marquand, A., Mourao-Miranda, J., Johnston, P., Daly, E. M., Brammer, M. J., … Murphy, D. G. (2010). Describing the brain in autism in five dimensions–magnetic resonance imaging-assisted diagnosis of autism spectrum disorder using a multiparameter classification approach. *Journal of Neuroscience*, *30*(32), 10612–10623. https://doi.org/10.1523/JNEUROSCI.5413-09.2010

Ecker, C., Rocha-Rego, V., Johnston, P., Mourao-Miranda, J., Marquand, A., Daly, E. M., … Consortium, M. A. (2010). Investigating the predictive value of whole-brain structural MR scans in autism: A pattern classification approach. *NeuroImage*, *49*(1), 44–56. https://doi.org/10.1016/j.neuroimage.2009.08.024

First, M. B., Williams, J. B. W., Karg, R. S., & Spitzer, R. L. (2015). *Structured clinical interview for DSM-5 disorders, clinician version (SCID-5-CV)*. Arlington, VA: American Psychiatric Association.

Fischl, B. (2012). FreeSurfer. *NeuroImage*, *62*(2), 774–781. https://doi.org/10.1016/j.neuroimage.2012.01.021

Fischl, B., Sereno, M. I., & Dale, A. M. (1999). Cortical surface-based analysis. II: Inflation, flattening, and a surface-based coordinate system. *NeuroImage*, *9*(2), 195–207. https://doi.org/10.1006/nimg.1998.0396

Han, X., Jovicich, J., Salat, D., van der Kouwe, A., Quinn, B., Czanner, S., … Fischl, B. (2006). Reliability of MRI-derived measurements of human cerebral cortical thickness: The effects of field strength, scanner upgrade and manufacturer. *NeuroImage*, *32*(1), 180–194. https://doi.org/10.1016/j.neuroimage.2006.02.051

Hardan, A. Y., Minshew, N. J., Harenski, K., & Keshavan, M. S. (2001). Posterior fossa magnetic resonance imaging in autism. *Journal of the American Academy of Child & Adolescent Psychiatry*, *40*(6), 666–672. https://doi.org/10.1097/00004583-200106000-00011

Helles, A., Gillberg, C. I., Gillberg, C., & Billstedt, E. (2015). Asperger syndrome in males over two decades: Stability and predictors of diagnosis. *Journal of Child Psychology and Psychiatry*, *56*(6), 711–718. https://doi.org/10.1111/jcpp.12334

Hollander, E., Anagnostou, E., Chaplin, W., Esposito, K., Haznedar, M. M., Licalzi, E., … Buchsbaum, M. (2005). Striatal volume on magnetic resonance imaging and repetitive behaviors in autism. *Biological Psychiatry*, *58*(3), 226–232. https://doi.org/10.1016/j.biopsych.2005.03.040

Ingalhalikar, M., Parker, D., Bloy, L., Roberts, T. P., & Verma, R. (2011). Diffusion based abnormality markers of pathology: Toward learned diagnostic prediction of ASD. *NeuroImage*, *57*(3), 918–927. https://doi.org/10.1016/j.neuroimage.2011.05.023

Jiao, Y., Chen, R., Ke, X., Chu, K., Lu, Z., & Herskovits, E. H. (2010). Predictive models of autism spectrum disorder based on brain regional cortical thickness. *NeuroImage*, *50*(2), 589–599. https://doi.org/10.1016/j.neuroimage.2009.12.047

Jovicich, J., Czanner, S., Han, X., Salat, D., van der Kouwe, A., Quinn, B., … Fischl, B. (2009). MRI-derived measurements of human subcortical, ventricular and intracranial brain volumes: Reliability effects of scan sessions, acquisition sequences, data analyses, scanner upgrade, scanner vendors and field strengths. *NeuroImage*, *46*(1), 177–192. https://doi.org/10.1016/j.neuroimage.2009.02.010

Kassraian-Fard, P., Matthis, C., Balsters, J. H., Maathuis, M. H., & Wenderoth, N. (2016). Promises, pitfalls, and basic guidelines for applying machine learning classifiers to psychiatric imaging data, with autism as an example. *Frontiers in Psychiatry*, *7*, 177. https://doi.org/10.3389/fpsyt.2016.00177

Kaufmann, W. E., Cooper, K. L., Mostofsky, S. H., Capone, G. T., Kates, W. R., Newschaffer, C. J., … Lanham, D. C. (2003). Specificity of cerebellar vermian abnormalities in autism: A quantitative magnetic resonance imaging study. *Journal of Child Neurology*, *18*(7), 463–470. https://doi.org/10.1177/08830738030180070501

Kuperberg, G. R., Broome, M. R., McGuire, P. K., David, A. S., Eddy, M., Ozawa, F., … Fischl, B. (2003). Regionally localized thinning of the cerebral cortex in schizophrenia. *Archives of General Psychiatry*, *60*(9), 878–888. https://doi.org/10.1001/archpsyc.60.9.878

Lenroot, R. K., & Giedd, J. N. (2010). Sex differences in the adolescent brain. *Brain and Cognition*, *72*(1), 46–55. https://doi.org/10.1016/j.bandc.2009.10.008

Levitt, J. G., Blanton, R. E., Smalley, S., Thompson, P. M., Guthrie, D., McCracken, J. T., … Toga, A. W. (2003). Cortical sulcal maps in autism. *Cerebral Cortex*, *13*(7), 728–735.

Libero, L. E., DeRamus, T. P., Lahti, A. C., Deshpande, G., & Kana, R. K. (2015). Multimodal neuroimaging based classification of autism spectrum disorder using anatomical, neurochemical, and white matter correlates. *Cortex*, *66*, 46–59. https://doi.org/10.1016/j.cortex.2015.02.008

Luckhardt, C., Jarczok, T. A., & Bender, S. (2014). Elucidating the neurophysiological underpinnings of autism spectrum disorder: New developments. *Journal of Neural Transmission*, *121*(9), 1129–1144. https://doi.org/10.1007/s00702-014-1265-4

Lugnegard, T., Hallerback, M. U., & Gillberg, C. (2015). Asperger syndrome and schizophrenia: Overlap of self-reported autistic traits using the autism-spectrum quotient (AQ). *Nordic Journal of Psychiatry*, *69*(4), 268–274. https://doi.org/10.3109/08039488.2014.972452

Morey, R. A., Selgrade, E. S., Wagner, H. R., 2nd, Huettel, S. A., Wang, L., & McCarthy, G. (2010). Scan-rescan reliability of subcortical brain volumes derived from automated segmentation. *Human Brain Mapping*, *31*(11), 1751–1762. https://doi.org/10.1002/hbm.20973

Nicolson, R., DeVito, T. J., Vidal, C. N., Sui, Y., Hayashi, K. M., Drost, D. J., … Thompson, P. M. (2006). Detection and mapping of hippocampal abnormalities in autism. *Psychiatry Research*, *148*(1), 11–21. https://doi.org/10.1016/j.pscychresns.2006.02.005

Nielsen, J. A., Zielinski, B. A., Fletcher, P. T., Alexander, A. L., Lange, N., Bigler, E. D., … Anderson, J. S. (2013). Multisite functional connectivity MRI classification of autism: ABIDE results. *Frontiers in Human Neuroscience*, *7*, 599. https://doi.org/10.3389/fnhum.2013.00599

Orru, G., Pettersson-Yeo, W., Marquand, A. F., Sartori, G., & Mechelli, A. (2012). Using support vector machine to identify imaging

biomarkers of neurological and psychiatric disease: A critical review. *Neuroscience & Biobehavioral Reviews*, *36*(4), 1140–1152. https://doi.org/10.1016/j.neubiorev.2012.01.004

Pedregosa, F., Varoquaux, G., Gramfort, A., Michel, V., Thirion, B., Grisel, O., … Duchesnay, E. (2011). Scikit-learn: Machine learning in Python. *Journal of Machine Learning Research*, *12*, 2825–2830.

Piven, J., Berthier, M. L., Starkstein, S. E., Nehme, E., Pearlson, G., & Folstein, S. (1990). Magnetic resonance imaging evidence for a defect of cerebral cortical development in autism. *American Journal of Psychiatry*, *147*(6), 734–739. https://doi.org/10.1176/ajp.147.6.734

Rosas, H. D., Liu, A. K., Hersch, S., Glessner, M., Ferrante, R. J., Salat, D. H., … Fischl, B. (2002). Regional and progressive thinning of the cortical ribbon in Huntington's disease. *Neurology*, *58*(5), 695–701.

Rubenstein, J. L., & Merzenich, M. M. (2003). Model of autism: Increased ratio of excitation/inhibition in key neural systems. *Genes, Brain and Behavior*, *2*(5), 255–267.

Ruzich, E., Allison, C., Smith, P., Watson, P., Auyeung, B., Ring, H., & Baron-Cohen, S. (2015). Measuring autistic traits in the general population: A systematic review of the autism-spectrum quotient (AQ) in a nonclinical population sample of 6,900 typical adult males and females. *Molecular Autism*, *6*, 2. https://doi.org/10.1186/2040-2392-6-2

Sabuncu, M. R., Konukoglu, E., & Alzheimer's Disease Neuroimaging Initiative. (2015). Clinical prediction from structural brain MRI scans: A large-scale empirical study. *Neuroinformatics*, *13*(1), 31–46. https://doi.org/10.1007/s12021-014-9238-1

Schumann, C. M., Hamstra, J., Goodlin-Jones, B. L., Lotspeich, L. J., Kwon, H., Buonocore, M. H., … Amaral, D. G. (2004). The amygdala is enlarged in children but not adolescents with autism; the hippocampus is enlarged at all ages. *Journal of Neuroscience*, *24*(28), 6392–6401. https://doi.org/10.1523/JNEUROSCI.1297-04.2004

Sheehan, D. V., Lecrubier, Y., Sheehan, K. H., Amorim, P., Janavs, J., Weiller, E., … Dunbar, G. C. (1998). The Mini-International Neuropsychiatric Interview (M.I.N.I.): The development and validation of a structured diagnostic psychiatric interview for DSM-IV and ICD-10. *Journal of Clinical Psychiatry*, *59*(Suppl. 20), 22–33.

Sparks, B. F., Friedman, S. D., Shaw, D. W., Aylward, E. H., Echelard, D., Artru, A. A., … Dager, S. R. (2002). Brain structural abnormalities in young children with autism spectrum disorder. *Neurology*, *59*(2), 184–192.

Uddin, L. Q., Menon, V., Young, C. B., Ryali, S., Chen, T., Khouzam, A., … Hardan, A. Y. (2011). Multivariate searchlight classification of structural magnetic resonance imaging in children and adolescents with autism. *Biological Psychiatry*, *70*(9), 833–841. https://doi.org/10.1016/j.biopsych.2011.07.014

Waterhouse, L., London, E., & Gillberg, C. (2017). The ASD diagnosis has blocked the discovery of valid biological variation in neurodevelopmental social impairment. *Autism Research*, *10*(7), 1182. https://doi.org/10.1002/aur.1832

Wechsler, D. (1999). *Wechsler abbreviated scale of intelligence (WASI)*. San Antonio, TX: Harcourt Assessment.

Wechsler, D. (2008). *Wechsler adult intelligence scale-IV*. San Antonio, TX: The Psychological Corporation.

Williams, J. H., Whiten, A., Suddendorf, T., & Perrett, D. I. (2001). Imitation, mirror neurons and autism. *Neuroscience & Biobehavioral Reviews*, *25*(4), 287–295.

World Health Organization. (1992). *The ICD-10 classification of mental and behavioral disorders: Clinical descriptions and diagnostic guidelines* (10th ed.). Geneva, Switzerland: World Health Organization.

Zhou, Y., Yu, F., & Duong, T. (2014). Multiparametric MRI characterization and prediction in autism spectrum disorder using graph theory and machine learning. *PLoS One*, *9*(6), e90405. https://doi.org/10.1371/journal.pone.0090405

SUPPORTING INFORMATION

Additional supporting information may be found online in the Supporting Information section at the end of this article.

How to cite this article: Sarovic D, Hadjikhani N, Schneiderman J, Lundström S, Gillberg C. Autism classified by magnetic resonance imaging: A pilot study of a potential diagnostic tool. *Int J Methods Psychiatr Res*. 2020;29:e1846. https://doi.org/10.1002/mpr.1846

APPENDIX A Subcortical volume (SCV) segmentation results

Region of interest	Laterality/part	ASD, mean ± SD (cm^3)	TD, mean ± SD (cm^3)	*p*-value
Brain stem	-	22.70 ± 2.4	21.28 ± 2.5	0.06
Cerebellum cortex	Left	55.75 ± 6.0	55.49 ± 5.8	0.88
	Right	57.71 ± 6.3	55.23 ± 5.7	0.18
Cerebellum white matter	Left	15.75 ± 2.3	16.32 ± 2.5	0.43
	Right	15.51 ± 2.6	16.11 ± 2.4	0.43
Corpus callosum	Anterior	0.92 ± 0.2	0.87 ± 0.2	0.33
	Mid-anterior*	0.51 ± 0.1	0.44 ± 0.1	0.04
	Central*	0.47 ± 0.1	0.40 ± 0.1	0.01
	Mid-posterior	0.46 ± 0.1	0.41 ± 0.1	0.05
	Posterior	1.00 ± 0.2	0.89 ± 0.2	0.11
Thalamus	Left*	8.43 ± 0.8	7.54 ± 1.2	0.007
	Right**	7.62 ± 0.7	6.85 ± 0.8	0.002
Caudate nucleus	Left*	4.12 ± 0.6	3.69 ± 0.6	0.03
	Right*	4.25 ± 0.7	3.83 ± 0.6	0.03

APPENDIX A (Continued)

Region of interest	Laterality/part	ASD, mean ± SD (cm^3)	TD, mean ± SD (cm^3)	*p*-value
Nucleus pallidus	Left**	1.78 ± 0.2	1.44 ± 0.3	0.0001
	Right*	1.75 ± 0.2	1.60 ± 0.2	0.04
Amygdala	Left*	1.65 ± 0.3	1.41 ± 0.4	0.02
	Right	1.79 ± 0.2	1.67 ± 0.4	0.22
Hippocampus	Left**	4.28 ± 0.5	3.69 ± 0.6	0.0007
	Right**	4.46 ± 0.5	3.66 ± 0.6	0.00002
Putamen	Left	6.30 ± 0.9	6.38 ± 0.6	0.74
	Right	5.97 ± 0.8	5.97 ± 0.8	0.98
Accumbens area	Left	0.67 ± 0.1	0.68 ± 0.1	0.84
	Right	0.66 ± 0.1	0.63 ± 0.1	0.47
Ventral diencephalon	Left	4.23 ± 0.4	4.00 ± 0.4	0.07
	Right*	4.20 ± 0.4	3.75 ± 0.6	0.004

Abbreviations: ASD, autism spectrum disorder; TD, typically developed.
*$p < 0.05$, **$p < 0.002$, **Significance level after Bonferroni correction within the family of SCV = 0.05/26 = 0.0019.

APPENDIX B Cortical thickness (Th) segmentation results

Region of interest	Laterality	ASD, mean ± SD (mm)	TD, mean ± SD (mm)	*p*-value
Caudal anterior cingulate	Left**	2.69 ± 0.3	2.25 ± 0.3	0.00002
	Right	2.40 ± 0.3	2.25 ± 0.3	0.07
Rostral anterior cingulate	Left**	2.91 ± 0.3	2.51 ± 0.3	0.0001
	Right*	2.71 ± 0.2	2.44 ± 0.3	0.002
Isthmus cingulate	Left	2.54 ± 0.3	2.39 ± 0.3	0.11
	Right	2.49 ± 0.2	2.38 ± 0.2	0.15
Posterior cingulate	Left	2.53 ± 0.2	2.41 ± 0.3	0.07
	Right*	2.51 ± 0.2	2.30 ± 0.3	0.004
Insula	Left	3.08 ± 0.1	2.98 ± 0.2	0.08
	Right	3.06 ± 0.2	2.98 ± 0.3	0.20
Lingual	Left*	2.10 ± 0.1	2.23 ± 0.2	0.05
	Right*	2.17 ± 0.2	2.24 ± 0.1	0.04
Fusiform	Left*	2.69 ± 0.2	2.56 ± 0.2	0.03
	Right**	2.79 ± 0.2	2.46 ± 0.2	0.000004
Entorhinal	Left**	3.29 ± 0.4	2.81 ± 0.4	0.0005
	Right**	3.28 ± 0.4	2.70 ± 0.4	0.0005
Parahippocampal	Left*	2.75 ± 0.3	2.43 ± 0.4	0.008
	Right**	2.75 ± 0.3	2.31 ± 0.4	0.0001
Precuneus	Left	2.40 ± 0.1	2.43 ± 0.2	0.58
	Right	2.45 ± 0.1	2.43 ± 0.1	0.75
Cuneus	Left*	1.96 ± 0.1	2.11 ± 0.2	0.004
	Right*	1.98 ± 0.2	2.15 ± 0.2	0.002

(Continues)

APPENDIX B (Continued)

Region of interest	Laterality	ASD, mean ± SD (mm)	TD, mean ± SD (mm)	*p*-value
Superior frontal	Left	2.68 ± 0.4	2.70 ± 0.1	0.78
	Right	2.65 ± 0.1	2.66 ± 0.2	0.79
Rostral middle frontal	Left	2.40 ± 0.2	2.38 ± 0.2	0.59
	Right*	2.25 ± 0.1	2.36 ± 0.2	0.05
Caudal middle frontal	Left	2.58 ± 0.1	2.56 ± 0.1	0.49
	Right	2.49 ± 0.2	2.52 ± 0.1	0.49
Lateral orbitofrontal	Left	2.65 ± 0.2	2.59 ± 0.2	0.29
	Right	2.54 ± 0.2	2.51 ± 0.2	0.61
Medial orbitofrontal	Left	2.41 ± 0.2	2.32 ± 0.1	0.08
	Right	2.28 ± 0.2	2.25 ± 0.2	0.43
Pars triangularis	Left	2.48 ± 0.1	2.46 ± 0.1	0.63
	Right	2.38 ± 0.1	2.50 ± 0.1	0.08
Pars opercularis	Left	2.69 ± 0.2	2.56 ± 0.1	0.31
	Right	2.52 ± 0.2	2.54 ± 0.2	0.86
Pars orbitalis	Left	2.78 ± 0.2	2.71 ± 0.2	0.34
	Right	2.58 ± 0.3	2.61 ± 0.3	0.70
Frontal pole	Left	2.60 ± 0.3	2.65 ± 0.2	0.47
	Right	2.64 ± 0.3	2.69 ± 0.3	0.87
Precentral	Left	2.59 ± 0.1	2.64 ± 0.1	0.54
	Right*	2.50 ± 0.2	2.60 ± 0.1	0.04
Paracentral	Left	2.43 ± 0.1	2.43 ± 0.2	0.97
	Right	2.43 ± 0.1	2.40 ± 0.1	0.43
Postcentral	Left	2.14 ± 0.1	2.19 ± 0.1	0.14
	Right	2.12 ± 0.1	2.17 ± 0.1	0.19
Supramarginal	Left	2.51 ± 0.2	2.55 ± 0.1	0.35
	Right	2.54 ± 0.4	2.55 ± 0.2	0.87
Banks of superior temporal sulcus	Left	2.43 ± 0.1	2.39 ± 0.2	0.44
	Right*	2.64 ± 0.2	2.50 ± 0.2	0.02
Inferior parietal	Left*	2.38 ± 0.1	2.47 ± 0.1	0.02
	Right	2.46 ± 0.1	2.50 ± 0.2	0.34
Superior parietal	Left*	2.20 ± 0.1	2.26 ± 0.1	0.05
	Right	2.21 ± 0.1	2.28 ± 0.1	0.05
Inferior temporal	Left*	2.65 ± 0.2	2.53 ± 0.2	0.04
	Right**	2.76 ± 0.2	2.43 ± 0.3	0.000001
Middle temporal	Left*	2.80 ± 0.2	2.61 ± 0.2	0.003
	Right*	2.88 ± 0.2	2.65 ± 0.2	0.0008
Superior temporal	Left*	2.79 ± 0.2	2.64 ± 0.2	0.009
	Right**	2.85 ± 0.2	2.65 ± 0.2	0.0005
Transverse temporal	Left	2.45 ± 0.3	2.53 ± 0.3	0.36
	Right	2.52 ± 0.3	2.58 ± 0.2	0.40

APPENDIX B (Continued)

Region of interest	Laterality	ASD, mean ± SD (mm)	TD, mean ± SD (mm)	*p*-value
Temporal pole	Left	3.50 ± 0.6	3.21 ± 0.4	0.06
	Right*	3.68 ± 0.5	3.16 ± 0.5	0.002
Pericalcarine	Left**	1.76 ± 0.2	1.97 ± 0.1	0.0002
	Right**	1.74 ± 0.2	2.02 ± 0.2	0.000005
Lateral occipital	Left*	2.11 ± 0.2	2.29 ± 0.2	0.0009
	Right	2.25 ± 0.2	2.35 ± 0.1	0.06

Abbreviations: ASD, autism spectrum disorder; TD, typically developed.
*$p < 0.05$, **$p < 0.0007$, **Significance level after Bonferroni correction within the family of Th = 0.05/68 = 0.00074.

APPENDIX C Cortical area (Ar) segmentation results

Region of interest	Laterality	ASD, mean ± SD (cm^2)	TD, mean ± SD (cm^2)	*p*-value
Caudal anterior cingulate	Left	7.11 ± 1.4	6.44 ± 1.0	0.07
	Right	8.85 ± 2.4	8.10 ± 1.4	0.21
Rostral anterior cingulate	Left*	8.99 ± 1.6	8.03 ± 1.3	0.03
	Right*	7.65 ± 1.4	6.65 ± 1.7	0.03
Isthmus cingulate	Left	11.44 ± 2.3	11.67 ± 2.1	0.73
	Right	10.20 ± 2.0	10.54 ± 1.9	0.56
Posterior cingulate	Left	12.83 ± 2.5	11.87 ± 1.3	0.12
	Right	13.15 ± 2.4	12.28 ± 1.3	0.15
Insula	Left	23.21 ± 4.1	21.77 ± 2.1	0.15
	Right*	23.65 ± 3.8	21.18 ± 3.0	0.02
Lingual	Left*	32.27 ± 4.7	29.38 ± 3.8	0.03
	Right*	32.23 ± 4.1	29.72 ± 3.8	0.04
Fusiform	Left	35.75 ± 3.3	33.29 ± 4.9	0.05
	Right	35.43 ± 4.8	32.00 ± 4.8	0.10
Entorhinal	Left	4.56 ± 1.2	4.16 ± 0.8	0.20
	Right*	3.85 ± 1.0	3.31 ± 0.8	0.05
Parahippocampal	Left	7.59 ± 1.3	7.11 ± 1.1	0.17
	Right	7.61 ± 1.2	7.01 ± 0.9	0.08
Precuneus	Left	41.52 ± 4.7	39.89 ± 4.7	0.25
	Right	43.42 ± 6.9	42.14 ± 5.6	0.50
Cuneus	Left	15.48 ± 1.7	14.41 ± 2.1	0.07
	Right	15.68 ± 2.1	15.48 ± 1.9	0.75
Superior frontal	Left	77.92 ± 9.1	76.51 ± 8.6	0.60
	Right	76.08 ± 9.2	74.05 ± 9.5	0.47
Rostral middle frontal	Left	62.72 ± 6.5	58.70 ± 8.0	0.07
	Right*	66.47 ± 8.0	59.40 ± 9.6	0.01
Caudal middle frontal	Left*	26.34 ± 4.8	23.50 ± 3.5	0.03
	Right	22.71 ± 4.6	22.17 ± 3.8	0.67
Lateral orbitofrontal	Left*	28.05 ± 4.0	24.36 ± 3.0	0.001
	Right*	27.99 ± 3.3	24.59 ± 3.8	0.003

(Continues)

APPENDIX C (Continued)

Region of interest	Laterality	ASD, mean ± SD (cm^2)	TD, mean ± SD (cm^2)	*p*-value
Medial orbitofrontal	Left	19.39 ± 2.5	18.82 ± 2.2	0.42
	Right	19.69 ± 2.8	18.72 ± 2.3	0.21
Pars triangularis	Left	13.56 ± 2.0	13.46 ± 2.1	0.87
	Right	15.87 ± 2.5	16.17 ± 2.6	0.70
Pars opercularis	Left	18.94 ± 4.0	17.52 ± 3.1	0.20
	Right	14.85 ± 2.4	14.22 ± 1.8	0.33
Pars orbitalis	Left	6.92 ± 0.7	6.56 ± 0.9	0.15
	Right*	8.68 ± 1.0	7.92 ± 1.4	0.04
Frontal pole	Left	2.39 ± 0.3	2.43 ± 0.3	0.65
	Right	3.15 ± 0.3	3.18 ± 0.5	0.84
Precentral	Left	52.01 ± 6.3	50.12 ± 4.6	0.27
	Right	53.66 ± 5.1	51.14 ± 4.2	0.08
Paracentral	Left	14.64 ± 2.4	14.44 ± 1.6	0.73
	Right	16.46 ± 2.8	16.31 ± 2.5	0.84
Postcentral	Left	46.38 ± 5.2	43.56 ± 4.2	0.05
	Right	43.72 ± 5.7	41.64 ± 4.5	0.19
Supramarginal	Left	43.17 ± 5.3	40.53 ± 4.5	0.08
	Right*	40.87 ± 6.4	37.11 ± 4.8	0.03
Banks of superior temporal sulcus	Left**	11.69 ± 2.0	9.68 ± 1.6	0.0007
	Right*	10.66 ± 1.3	9.43 ± 1.6	0.008
Inferior parietal	Left	50.39 ± 5.4	47.03 ± 8.1	0.10
	Right	61.01 ± 8.5	57.99 ± 8.5	0.24
Superior parietal	Left	57.73 ± 5.8	57.02 ± 5.5	0.68
	Right	58.22 ± 5.5	57.23 ± 6.4	0.58
Inferior temporal	Left**	38.27 ± 4.3	31.84 ± 5.6	0.00009
	Right**	37.15 ± 4.6	31.01 ± 5.8	0.0003
Middle temporal	Left*	34.74 ± 4.0	30.76 ± 4.3	0.002
	Right*	39.59 ± 4.7	33.70 ± 4.7	0.001
Superior temporal	Left	40.62 ± 4.9	38.31 ± 4.4	0.11
	Right	38.31 ± 4.7	36.06 ± 4.3	0.10
Transverse temporal	Left	4.77 ± 0.8	4.54 ± 0.7	0.32
	Right	3.68 ± 0.7	3.44 ± 0.5	0.20
Temporal pole	Left	5.11 ± 0.8	5.49 ± 0.5	0.06
	Right	4.44 ± 0.8	4.35 ± 0.7	0.71
Pericalcarine	Left	13.62 ± 2.4	12.67 ± 2.3	0.18
	Right	15.28 ± 2.5	13.98 ± 2.5	0.09
Lateral occipital	Left	52.15 ± 6.0	49.84 ± 5.1	0.17
	Right*	51.06 ± 6.1	46.79 ± 4.5	0.01

Abbreviations: ASD, autism spectrum disorder; TD, typically developed.

*$p < 0.05$, **$p < 0.0007$, **Significance level after Bonferroni correction within the family of Ar = 0.05/68 = 0.00074.

APPENDIX D White matter (WM) segmentation results

Region of interest	Laterality	ASD, mean ± SD (cm^3)	TD, mean ± SD (cm^3)	*p*-value
Caudal anterior cingulate	Left	3.03 ± 0.5	2.81 ± 0.4	0.10
	Right*	3.46 ± 0.7	3.11 ± 0.4	0.05
Rostral anterior cingulate	Left	2.87 ± 0.5	2.73 ± 0.6	0.36
	Right	2.43 ± 0.4	2.18 ± 0.4	0.03
Isthmus cingulate	Left	4.22 ± 0.7	4.23 ± 0.8	0.96
	Right	3.79 ± 0.6	3.74 ± 0.7	0.80
Posterior cingulate	Left*	4.84 ± 0.6	4.45 ± 0.4	0.02
	Right	4.75 ± 0.8	4.39 ± 0.5	0.07
Insula	Left*	9.04 ± 1.6	8.14 ± 0.9	0.03
	Right*	9.33 ± 1.7	7.93 ± 1.1	0.002
Lingual	Left*	5.95 ± 1.0	5.06 ± 0.7	0.002
	Right*	5.96 ± 1.0	5.13 ± 0.9	0.008
Fusiform	Left	7.33 ± 0.7	6.80 ± 1.4	0.10
	Right	7.25 ± 0.9	6.77 ± 1.2	0.14
Entorhinal	Left	0.95 ± 0.3	0.80 ± 0.2	0.07
	Right*	0.78 ± 0.2	0.62 ± 0.2	0.007
Parahippocampal	Left*	1.78 ± 0.3	1.57 ± 0.3	0.03
	Right*	1.95 ± 0.4	1.59 ± 0.3	0.002
Precuneus	Left	10.13 ± 1.4	9.59 ± 1.3	0.18
	Right	10.80 ± 1.8	10.19 ± 1.6	0.23
Cuneus	Left*	2.57 ± 0.4	2.25 ± 0.5	0.02
	Right	2.52 ± 0.4	2.31 ± 0.4	0.09
Superior frontal	Left	19.37 ± 2.3	18.82 ± 2.3	0.43
	Right	18.81 ± 2.0	18.07 ± 3.4	0.37
Rostral middle frontal	Left	13.61 ± 1.6	12.80 ± 1.9	0.14
	Right*	14.25 ± 2.2	12.68 ± 2.3	0.03
Caudal middle frontal	Left	7.39 ± 1.2	6.82 ± 1.0	0.10
	Right	6.17 ± 1.1	5.87 ± 1.1	0.36
Lateral orbitofrontal	Left*	7.13 ± 1.0	6.37 ± 0.9	0.009
	Right*	7.17 ± 0.9	6.57 ± 1.0	0.04
Medial orbitofrontal	Left	3.77 ± 0.7	3.78 ± 0.6	0.94
	Right	3.72 ± 0.5	3.74 ± 0.5	0.91
Pars triangularis	Left	3.08 ± 0.5	3.16 ± 0.6	0.59
	Right	3.46 ± 0.6	3.52 ± 0.5	0.73
Pars opercularis	Left	4.09 ± 0.9	3.76 ± 0.8	0.21
	Right	3.55 ± 0.7	3.32 ± 0.4	0.16
Pars orbitalis	Left	0.99 ± 0.1	0.91 ± 0.1	0.09
	Right*	1.31 ± 0.2	1.18 ± 0.3	0.11
Frontal pole	Left	0.25 ± 0.1	0.25 ± 0.1	0.89
	Right	0.34 ± 0.1	0.34 ± 0.1	0.83

(Continues)

APPENDIX D (Continued)

Region of interest	Laterality	ASD, mean ± SD (cm^3)	TD, mean ± SD (cm^3)	*p*-value
Precentral	Left	13.53 ± 3.1	13.49 ± 1.7	0.96
	Right	13.88 ± 2.5	14.01 ± 1.6	0.84
Paracentral	Left	3.97 ± 0.7	4.08 ± 0.6	0.61
	Right	4.81 ± 1.0	5.04 ± 0.8	0.39
Postcentral	Left	8.36 ± 1.1	7.75 ± 0.9	0.05
	Right	8.05 ± 1.2	7.61 ± 1.1	0.21
Supramarginal	Left	9.40 ± 1.4	8.93 ± 1.2	0.23
	Right	9.54 ± 1.6	8.83 ± 1.4	0.12
Banks of superior temporal sulcus	Left*	32.4 ± 0.8	25.4 ± 0.7	0.004
	Right*	3.13 ± 0.5	2.77 ± 0.7	0.05
Inferior parietal	Left	10.92 ± 1.4	9.92 ± 1.7	0.04
	Right	13.03 ± 2.0	12.23 ± 1.7	0.16
Superior parietal	Left	13.02 ± 1.6	12.17 ± 2.5	0.17
	Right	12.66 ± 1.6	12.13 ± 2.0	0.33
Inferior temporal	Left*	7.06 ± 0.8	6.05 ± 1.3	0.002
	Right*	6.79 ± 0.8	58.1 ± 1.3	0.004
Middle temporal	Left*	5.79 ± 0.8	5.25 ± 0.9	0.04
	Right*	6.73 ± 0.8	5.93 ± 1.2	0.01
Superior temporal	Left	8.29 ± 1.3	7.89 ± 1.1	0.27
	Right	7.18 ± 1.2	6.75 ± 0.9	0.20
Transverse temporal	Left	0.86 ± 0.2	0.82 ± 0.1	0.42
	Right	0.61 ± 0.1	0.60 ± 0.1	0.83
Temporal pole	Left*	0.76 ± 0.1	0.85 ± 0.1	0.02
	Right	0.70 ± 0.2	0.70 ± 0.2	0.98
Pericalcarine	Left	3.24 ± 0.8	2.92 ± 0.6	0.13
	Right*	3.39 ± 0.7	2.87 ± 0.6	0.01
Lateral occipital	Left	9.85 ± 1.3	9.23 ± 1.3	0.12
	Right*	9.94 ± 1.5	8.73 ± 1.2	0.005

Abbreviations: ASD, autism spectrum disorder; TD, typically developed.
*$p < 0.05$.